

IMAGE SEGMENTATION BASED ON G-UN-MMS AND HEURISTICS. THEORETICAL BACKGROUND AND RESULTS

Horia-Nicolai TEODORESCU^{1,2}, Mariana RUSU³

¹“Gheorghe Asachi” Technical University of Iasi, 8 Bd. Carol, Iasi Romania,

² Institute of Computer Science of the Romanian Academy, Iasi, Romania

³ Technical University of Moldova, R. Moldova, Chisinau, Bd. Stefan cel Mare, 168

E-mail: hteodor@etti.tuiasi.ro

We present the concept of image segmentation based on Gauss - Uniform Noise Mixed Models (G-UN-MM) that we also introduce in this paper, the theoretical foundation of the segmentation method based on this model, results of the method on several classes of pictures, and a comparison with other methods. The proposed implementation of the G-UN-MM method has a simple and sound theoretical foundation and is not computationally demanding. It produces in many cases better segmentation results than other methods that are more computationally intensive.

Key words: image segmentation, statistical model, Gauss mixed model, uniform noise mixed model, histogram, algorithm, heuristic rules.

1. INTRODUCTION

Robotics and automatic information processing have persistently pushed forward the domain of image processing during more than five decades already. Since the 1970s, methods for image segmentation have emerged in view of automatic image recognition and understanding. There is a huge and ever increasing number of papers on image segmentation. Several review papers, as [1–5] sum up the evolution of the domain and the vast collection of methods proposed for image segmentation.

However, after decades of progress, image segmentation remains an issue of intense research. Various approaches to image segmentation produce very good results for relatively well-defined objects in the image, where the definition is understood in terms of a set of specified features, like color, brightness, or texture. No segmentation method performs well enough on all classes of images. Even human experts produce very different segmentations when viewing the same picture [5].

2. THE G-UN-MM MODEL

The Gauss Mixed Models (GMM) are well established tools in the literature, with applications in image and speech processing and in data clustering. The GMM model applied to histograms of the images lead to the well-known ‘valley’ method of segmentation. More developed segmentation methods based on histograms are presented for example in [6], [7], [8], and [9]. The common algorithms for determining the GMM models are highly sensitive to observational noise [10] and produce model solutions that are not guaranteed optimal. The same remains true for uniform noise mixed models (UNMM), because the model finding procedures are essentially the same. Therefore, we prefer an expeditious procedure for determining reasonable Gauss-uniform noise- mixed models, G-UN-MMs. The procedure employs heuristic rules and a set of parameters that can be adjusted during a supervised learning phase.

Recall that a GMM model (exemplified here for the single variable case) consists of an approximation of a given probability distribution $p(x)$ by a weighted sum (weights A_k) of normal distributions, $G_k(x)$, as

$$p(x) = \sum_{k=1}^{\infty} A_k \cdot G_k(x), \text{ where } G_k(x) = \frac{1}{\sqrt{2} \cdot \sigma_k} \cdot \exp\left(-\frac{(x - a_k)^2}{2 \cdot \sigma_k^2}\right). \quad (1)$$

Similarly, a UNMM model is defined as $p(x) = \sum_{h=1}^{\infty} B_h \cdot U_h(x)$, where $U_h(x) = \text{constant}$, $\forall x \in J_h \subset J$

and J_h are closed intervals. The segmentation method based on the ‘valleys’ in the image histogram is founded on the assumption that the histogram is well modeled by a GMM, moreover on the assumption that all segments in the image have normal distributions. In the literature, the first hypothesis is rarely clarified, or even mentioned; it actually says that the equation (1) reduces, up to a small error, ε , to

$$p(x) \approx \sum_{k=1}^N A_k \cdot G_k(x), \quad (2)$$

where N is small, typically less than 10, while ε represents a small fraction of the whole ‘energy’ $E = \int_J p^2(x) dx$ of the approximated function,

$$\int_J (p(x) - \sum_{k=1}^N (A_k \cdot G_k(x)))^2 dx < \varepsilon \cdot \int_J p^2(x) dx, \quad (3)$$

and J is the bounded interval of interest (for gray images, $J = [0, 255]$). With the above condition not met, there is little real reason to use a GMM for approximating the histogram, as other families of non-Gaussians functions can perform better in approximating the given function (that is, $p(x)$) with a finite sum of functions. The difficulty is to ‘guess’ a suitable family of such functions.

Many images have histograms that hardly verify the two hypotheses, which explains why the segmentation of these images, based on the ‘valleys’ in the histogram, perform poorly. As a matter of example, the image in Fig. 1 (left) has the far-from-GMM type histogram shown in Fig. 1(right). Instead, it is much easier to approximate it by the G-UN-MM model advocated in this paper.

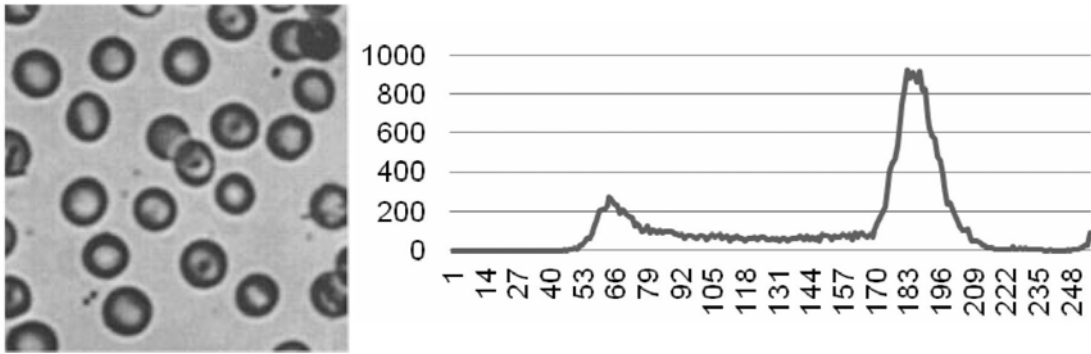


Fig. 1 – Example of histogram that is difficult to represent by a Gauss mixture model. Image of red cells from PUDN [15].

A true mixture of uniform and normal distribution functions may look composed of more Gauss functions than the case is, as in Fig. 2, where it may seem that two normal distributions overlap at lower values of x , while the effect is due to the superposition of a Gauss function (average 28, spreading 19) and a constant function (with value 0.028 in the interval 0 to 24). Similarly, the noisy function in Fig. 2 middle would need at least four Gauss functions to approximate the parts of the function between 0 and 40, respectively between 150 and 200), but the graph is actually that of a mixture of Gauss and constant functions, as seen in Fig. 2, right. Notice that the graph of the noisy function in the middle panel in Fig. 2 is vertically-translated; it represents the graph of the histogram before smoothing.

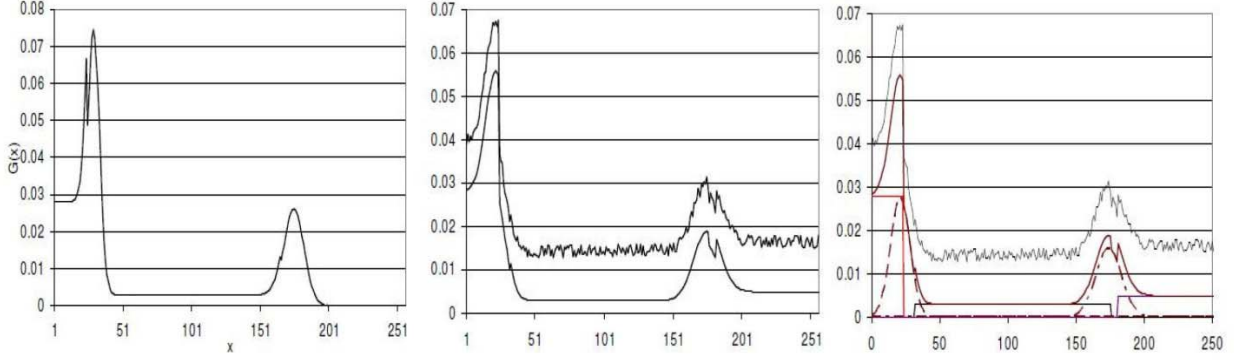


Fig. 2 – Examples of noisy Gauss and constant function mixtures that may falsely seem to be Gauss mixtures. A sum of three constant functions (seen like rectangles) and of two Gauss functions (represented by dotted lines), see the right panel, produce the distribution seen in the middle panel. Ox axis represents gray levels; vertical axis stands for histogram values.

We propose a more flexible model that extends GMM by including uniform distribution in the mixture, according to

$$p(x) = \sum_{k=1}^{\infty} A_k \cdot G_k(x) + \sum_{h=1}^{\infty} B_h \cdot U_h(x), \quad (4)$$

where A_k, B_h are constants, $U_h(x) = 1$ for $x \in J_h = [a_h, b_h]$, and $U_h(x) = 0$ elsewhere (that is, U_h are constant in their specific interval $[a_h, b_h]$). Accordingly, we propose the approximation

$$\left\| p(x) - \sum_{k=1}^{M_\varepsilon} A_k \cdot G_k(x) - \sum_{h=1}^{N_\varepsilon} B_h \cdot U_h(x) \right\| < \varepsilon, \quad (5)$$

where M_ε and N_ε are the minimal values that satisfy the condition and depend on ε , which determines the truncation.

Remark. Any derivable distribution with bounded derivative on a closed interval $J \subset R$ can be approximated according to equ. (5).

Proof. Directly results by combining the validity of staircase approximation, which results from Rolle (mean value) theorem, and the theorem on GMMs as universal approximators.

3. SEGMENTATION PROCEDURE

The first stage of the procedure is preprocessing, consisting in the removal of noise using a combined median and average filtering on 3x3 windows. The second stage is the determination of the histogram, followed by the third stage, which is the smoothing of the histogram, again by applying a set of median and average filters.

The smoothed histogram $H(x)$ is then approximated by a G-UN-MM either using one of the well-known techniques, as genetic algorithms (GA) or gradient descent, or a heuristic method. In this paper, we present the later version, for reasons that will become apparent subsequently.

The approximation is performed by searching first for the intervals where the function $H(x)$ is ‘almost’ constant, in the sense that on the specified interval its variation is less than a given constant percentage δ of the total variation of the function $H(x)$. In addition, we look for such intervals that have the maximal length. That is, we seek the maximal intervals $J_h \subset J$ satisfying the condition (i) $\forall x_1, x_2 \in J_h, |H(x_1) - H(x_2)| < \delta$. The problem setting is still imperfectly defined. In the first place, it is possible that there are many intervals $J_h = [a_h, b_h]$ satisfying the condition (i), but their length, $L(J_h) = L_h = b_h - a_h$, be very small, at the limit a_h, b_h corresponding to two successive gray levels in the image. For practical reasons, we

wish to impose the condition (ii) $L_h \geq \theta$ where θ is a specified value expressed in percentage of the gray scale, for example $\theta = 15\%$ of $G_{\max} = 255$; define $\Theta = 255 \cdot \theta$. On the other hand, the problem is not suitably defined, because the solution consisting in the set of intervals satisfying (i) and (ii) is not unique. This is easy to see considering a symmetric function, for example a parabola, with parts of both branches present in the interval of interest of the variable x : there are two intervals, placed symmetrically with respect to the parabola axis, which satisfy the conditions.

To remove multiple solutions, we require a third, constructive condition, namely (iii) the intervals are constructed starting with the lowest x value, each interval being determined by the conditions

$$(a) \ a_{h+1} > b_h$$

and

$$(b) \ a_{h+1} = \min_{x > b_h} (x \mid \forall x_1, x_2 \in [H(x), H(x + \Theta)], |H(x_1) - H(x_2)| < \delta). \quad (6)$$

We accelerate the interval search procedure by using a window W of length of about $\Theta/4$ and moving it from left to right with a step larger than 2 gray levels, for example a step of $W/2$. As long as the interval extended by the points in the new window satisfies the condition $\forall x_1, x_2 \in [H(x), H(x + \Theta)], |H(x_1) - H(x_2)| < \delta$ we keep growing the interval. The procedure determines a well defined set of intervals J_h that have no point in common. The set of points $a_1, b_1, a_2, b_2, \dots, a_q, b_q$, defining the intervals $[a_1, b_1], [a_2, b_2], \dots, [a_q, b_q]$, determined as above, is used as set of thresholds for the segmentation.

We can further simplify and significantly accelerate the procedure for finding the segmentation thresholds by relaxing the condition (5). Namely, we replace it with the condition that in every window W the function variation is limited, $\forall x_1, x_2 \in W, |H(x_1) - H(x_2)| < \delta$. In the simulations reported here, we used this simplified condition. The almost constant intervals were determined using an overlapping window of 24 samples considering the following rule: if $(V_{\max} - V_{\min}) = N_w < 1.5$, ($\delta = 1.5$), then the interval is considered constant, where $V_{\max} = \max_{x \in W} H(x)$ and $V_{\min} = \min_{x \in W} H(x)$ are the maximum and minimum values in the window W , and N_w is the number of samples in the window. If two successive windows have this property, we join them in the same interval. Else, the interval is considered non-constant (not representing a UN distribution). Notice that, according to this procedure, the threshold Θ is represented by the width of the window used to determine the (minimal length) intervals.

It is worth discussing the operation of the procedure described above. It can be viewed as a procedure for the detection of plateaus of the histogram, where the plateaus are the intervals $[a_h, b_h]$. For a ‘nicely’ behaving histogram, the procedure produces a reasonable detection of the Gauss and plateau (uniform noise) intervals, see Fig. 3. However, this is not always the case. Notice in Fig. 3 that the procedure identifies approximately the UN regions, while the Gauss regions are left apart. The intervals determined by the partition so produced will serve for segmentation and will work correctly for this task.

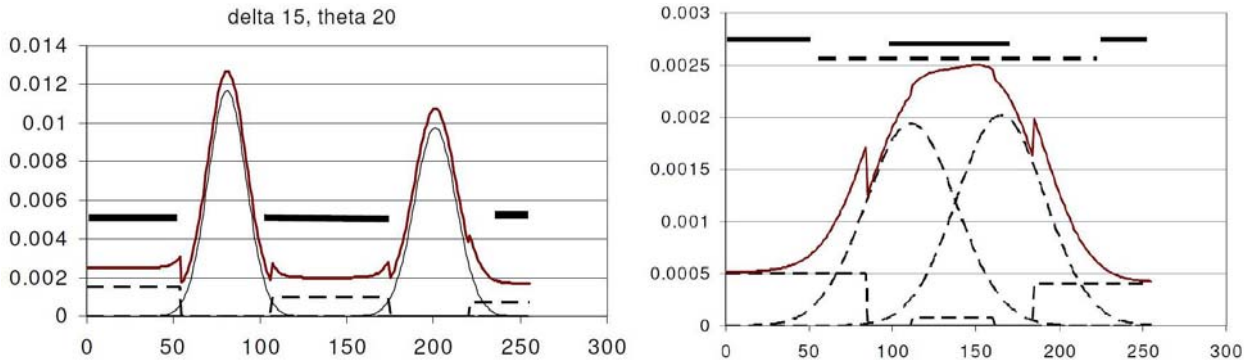


Fig. 3 – a) Intervals (marked by bars) detected for a nicely behaving histogram and for well chosen procedure parameters; b) intervals detected for a not so nicely behaving histogram; a plateau is determined in the region where the two Gauss functions superpose. Horizontal axis: gray levels; vertical axis: histogram values.

When the constant θ is large, the peaks of some Gaussians may be detected as plateaus. In addition, the region where two Gaussians with close averages superpose may be detected as plateaus. This is a significant difference to what a GMM would produce and may be a drawback in some cases. However, the limit is removed by taking smaller values for θ . Another difference between the segmentation produced by this procedure and a true GMM or a G-UN-MM is that the slopes of the Gauss functions may be detected as independent intervals. In this case, the results do not conform to a G-UN-MM. To remove at least partly this drawback, we introduce a couple of heuristic rules:

(Rule 1) If the interval before a plateau interval has a positive slope and the interval after the plateau has a decreasing slope, then the slopes are merged with the plateau interval.

(Rule 2) If a plateau interval is followed by a slope that has not to be merged with the next plateau, than the slope corresponds to a boundary between segments and objects and is equally divided between the adjacent plateaus. The effect of these rules will be partly illustrated in the Results section.

Figure 4b shows, in contrast to Fig. 4a, the sketch of a situation when the histogram is not a well-behaved one, with Gauss functions with large values of the spreading superposing and creating, together with some small amplitude uniform distribution, a plateau between them. The procedure selects the three intervals marked by thick solid lines. Applying the rules above, the result would be the formation of the larger interval marked by thick dotted lines.

4. RESULTS

We exemplify the operation of the procedure and the results for a few typical images. The images are from the public academic databases referred in the legends of the respective figures or in the text. The set of databases used comprises Berkeley Segmentation Dataset and Benchmark [11, 12], and SIPI database [13].

The histograms for images “rice” and “Lena” are shown in Fig. 5. Notice that both histograms appear to be mixtures of Gauss functions and plateaus, but that they are very different in complexity. The rice image has a very simple single-Gauss single-plateau structure.

In contrast, Lena histogram includes seven visually identifiable Gauss functions. In addition, it includes four plateaus that are easy to guess visually; two of these plateaus have almost null value and two (from about 70 to about 100, respectively from about 170 to about 200) have large swings around the average value in the interval. The segmented images produced by the described procedure are shown in Fig. 5 (NB. The “rice” image is from [17]; the image Lena is from SIPI Image Database – Misc [13]. The image of red cells used in Fig. 1 is from [15] and appears in numerous other papers. We believe that the images are copyright-free.)

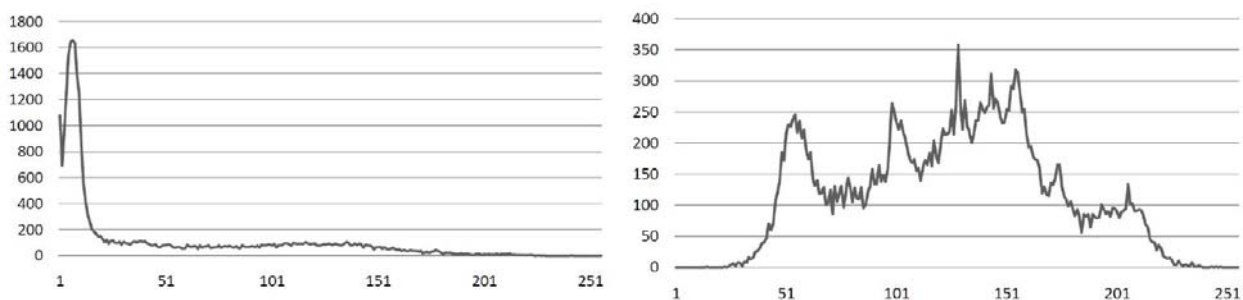


Fig. 4 – Histograms for the images “rice” (left) and “Lena” (right). Axes as in Fig. 3. Vertical “axes” number of pixels.

Notice in the segmented images in Figure 5 that, as expected, the algorithm detects for “Lena” a large number of thresholds (six). The segmentation obtained using the presented method, as in Fig. 5, compares favorably with the ones obtained in [14] and in [17], for Lena image, respectively with the results reported in [16] and [17], for “rice” image.

A more intricate image seems to be Fig. 6, which is not in the public domain. The picture represents giraffes in the wild and is difficult to segment even for the humans because of the similarity of shades of the animals and of the vegetation in the background, moreover because of the shadows. The histograms of the

original and filtered images, which are also given in Fig. 6, show that at least two Gauss functions and at least two or three almost-plateaus are present, one of them – a small one – at the peak of the first Gauss function. The segmented image is clearly selecting two of the giraffes, with the third giraffe partly visible too (see [18] for a discussion of these pictures).



Fig. 5 Segmentation of the “rice” and “Lena” images. Upper row: left – original; middle – segmented with two thresholds, right – segmented with one threshold. Lower row: left – original; right – segmented with six thresholds.

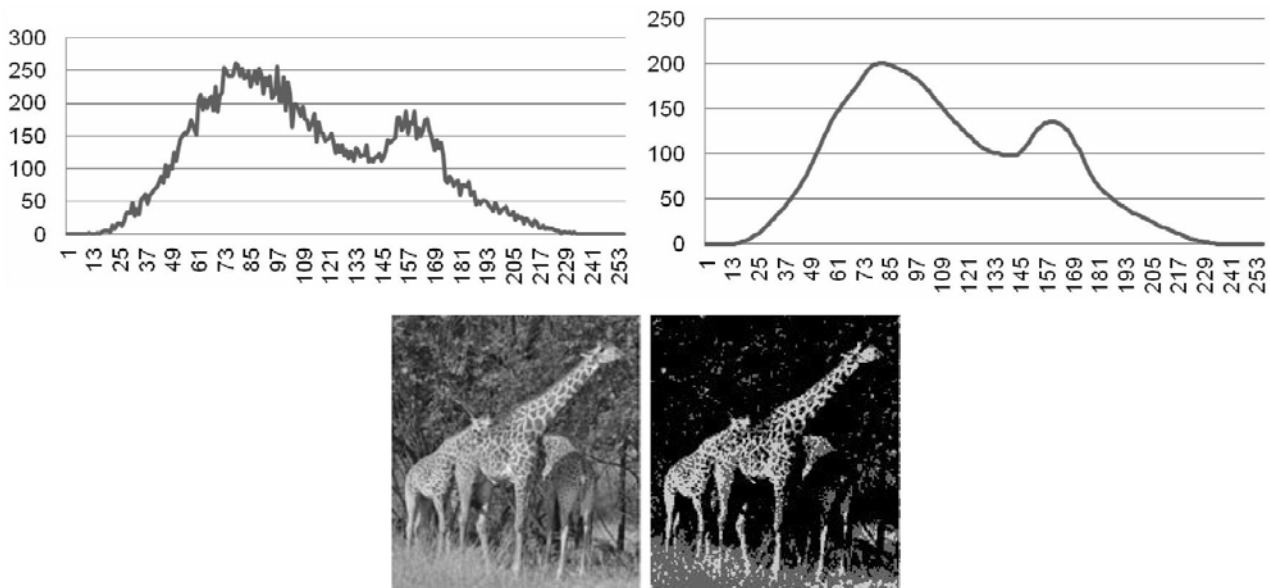


Fig. 6 – Histograms (upper panel: left – original, right filtered; axes variables as in Fig. 3), original and segmented image (lower panel). Original image graciously provided by Prof. Fred F. B. Bercovitch. Copyright remains with Prof. Bercovitch.

More segmentation results were published in two preliminary papers, [19], [20]. We also tested the influence of noise on the segmentation. Images with a SNR (signal to noise ratio) larger than 10 dB are virtually unaffected by additive uniform noise. A subsequent paper will present the analysis of the results on segmentation of noisy images.

4. DISCUSSION

The presented segmentation method is an improvement over the simple Gauss-model based segmentation, but it is not a universal method. When the histogram of the image is not easy to approximate by a G-UN mixed model, the method works poorly, as any other not-adapted model would do. Yet, even in the last case, the method is more capable of performing the approximation than a pure Gauss mixture model. The method proposed is not computationally demanding and compares well from this point of view to other methods, including those presented in the papers [21], [22], and [23]. Also, the method is easy to extend to multispectral images like those used in [24].

As any well-adapted to image segmentation method, when the model G-UN-MM is suitable, it may be used to compress information. Indeed, the loss of information when the pixels belonging to a given segment are replaced by a constant gray level is minimal to the human eye. Hence, for an image with q segments, replacing the 0 to 255 gray scale by a compressed scale of r levels, where $q < 2^r$, $r = \lceil \log_2 q \rceil$ will reduce the data in the image representation by a factor of $8/r$. For a color image, the reduction is $(8/r)^3$. For a gray scale picture, the reduction is typically to 3 or 4 bits instead of 8, leading to a 2:1 to 2.66:1. An example of compressed image is shown in Fig. 5 (Lena). The G-UN mixed model is not a knowledge-based one; therefore, we cannot expect that the segmentation based on G-UN-MM performs as a human segmenter. However, the model may help better detect segments that are meaningful to humans. The method can work as a supervised procedure if the value of the parameter ϵ and the number of allowed segments are not fixed by the user, but are optimized based on a set of images that have been segmented by human operators.

5. CONCLUSIONS AND FUTURE WORK

We have proposed a novel segmentation method that is based on the statistics of gray levels and on statistical considerations expressed as heuristic rules. For the foundation of the method, we introduced the Gauss-Uniform Noise Mixture Model that better fits than the Gauss Mixture Model the statistics of many images. Then, we exposed a segmentation algorithm based on the principles of G-UN-MMs. The algorithm determines directly, heuristically and approximately the intervals that the exact G-UN-MM would produce. The procedure has the advantage to be almost insensitive to noise and to departures from the ideal Gauss and uniform distributions. In addition, the procedure is not as computationally demanding as typical algorithms for GMMs and GUNMM are. While the procedure may work unsupervised, it needs a set of parameters with specified values. The procedure is easy to transform into a supervised one, where the parameters are adjusted automatically based on a set of images and on their ‘ideal’ segments. The exemplified results obtained for several images favorably compare to other results in the literature. While we can confidently say that there is no ideal segmentation procedure, because there are several criteria of segmentation performance evaluations, depending on the purpose of segmentation, we believe the segmentation method based on G-UN-MMs are a useful addition to the set of procedures and that it advances the capabilities of segmentation for a vast class of images.

We believe that the procedure is well suited for small portable equipment; due to the simple computations required by the procedure, it will reduce the power consumption and the computation time. In addition, the heuristic procedure presented is less sensitive to noise in the images and poses no stability issues. Embedding simple data mining capabilities in equipment for telemedicine, and ambulatory automated diagnostic equipment could benefit of this segmentation techniques, as would visual monitoring of wild animals in their habitats.

ACKNOWLEDGMENTS

We thank several colleagues, including Dr. M. Hulea, Mr. S. Bejinariu, Mr. Adrian Ciobanu, and Dr. Alina Hulea, for their comments and suggestions. The paper was not supported by any institution; it was benevolently performed by HNT and MR. The work supports the research in the frame of the Romanian Academy, especially the fundamental research project Cognitive Systems and the MIVIEM and MIACSAM

collaborations with the Institute for Mathematics and Computer Science of the Academy of Science of the R. Moldova (MIVIEM and MIACSAM grants). MR acknowledges the support of a grant from AUF.

Authors' contributions. HNT proposed the topic, the method of solving the segmentation, the models, the stages and main steps of the algorithms, some of the pictures for processing, interpreted most of the results and derived conclusions, wrote the paper, set in motion the writing of the code and corrected it. The GM-UN-MM models and method are entirely due to HNT. MR wrote the code, performed simulations and experiments, contributed to the interpretation of the results, and alone produced the largest part of processed images. The relative contributions of the authors is about 2/3 by HNT and 1/3 by MR. Both authors discussed the paper and agreed with its final form.

REFERENCES

1. N.R. PAL, S.K. PAL, *A Review on Image Segmentation Techniques*. Pattern Recognition, **26**, 9, pp. 1277–1294, 1993.
2. H.D. CHENG, X.H. JIANG, Y. SUN, J.L. WANG, *Color Image Segmentation: Advances and Prospects*, Pattern Recognition, **34**, 12, pp. 2259–2281, 2001.
3. T. HEIMANN, H.-P. MEINZER, *Statistical Shape Models for 3D Medical Image Segmentation: A review*, Medical Image Analysis, **13**, 4, pp. 543–563, 2009.
4. H. MUELLER, N. MICHOUX, D. BANDON, A. GEISSBUHLER, *A Review of Content-based Image Retrieval Systems in Medical Applications Clinical Benefits and Future Directions*. Int. J. Medical Informatics, **73**, p. 123, 2004.
5. P. ARBELAEZ, M. MAIRE, C. FOWLKES, and J. MALIK, *Contour Detection and Hierarchical Image Segmentation*, IEEE Trans. Pattern Anal. Mach. Intell. **33**, 5, pp. 898–916, 2011.
6. J. ZHANG and J. HU, *Image Segmentation Based on 2D Otsu Method with Histogram Analysis*, 2008 Int. Conf. on Computer Science and Software Engineering, IEEE, DOI 10.1109/CSSE.2008.206, pp. 105–108, 2008.
7. O.J. TOBIAS and R. SEARA, *Image Segmentation by Histogram Thresholding Using Fuzzy Sets*, IEEE Trans. Image Processing, **11**, 12, pp. 1457–1465, 2002.
8. A. KHOTANZAD and A. BOUARFA, *Image Segmentation by A Parallel, Nonparametric Histogram Based Clustering Algorithm*, Pattern Recognition, **23**, 9, pp. 961–973, 1990.
9. F. KURUGOLLU, B. SANKUR and A.E. HARMANCI, *Color Image Segmentation using Histogram Multithresholding and Fusion*, Image Vision Comput., **19**, 13, pp. 915–928, 2001.
10. J. HAO et al., *Precision Measurements of the Cluster Red Sequence Using an Error-Corrected Gaussian Mix-ture Model*, The Astrophysical Journal, doi:10.1088/0004-637X/702/1/745 2009, **702**, pp. 745758, 2009.
11. MARTIN, C. FOWLKES, D. TAL, and J. MALIK, *A Database of Human Segmented Natural Images and its Application to Evaluating Segmentation Algorithms and Measuring Ecological Statistics*, Proc. 8th Int'l Conf. Computer Vision, 2001, pp. 416–423.
12. *** The Berkeley Segmentation Dataset and Benchmark. Image #61086, <http://www.eecs.berkeley.edu/Research/Projects/CS/vision/bsds/>, <http://www.eecs.berkeley.edu/Research/Projects/CS/vision/bsds/BSDS300/html/dataset/humans/1113-0001-0010.html>
13. *** The USC-SIPI Image Database. <http://sipi.usc.edu/database/database.php>. Signal and Image Processing Institute, University of Southern California, USC Viterbi, SIPI Image Database - Misc., <http://sipi.usc.edu/database/>
14. Z. PAN, L. CHEN, G. ZHANG, *Threshold Segmentation using Cultural Algorithms for Image Analysis*, International Symposium on Photoelectronic Detection and Imaging 2007: Related Technologies and Applications, Proc. SPIE 6625, 662512, 2007.
15. *** The blood cells <http://www.pudn.com/downloads58/sourcecode/math/detail206012.html>
16. Y.B. CHEN, *A robust fully automatic scheme for general image segmentation*, Digital Signal Processing, **21**, pp. 8799, 2011.
17. S.M. PRASAD, D.T. S.B. RAO, N.C. RAJU, *Unsupervised Image Thresholding using Fuzzy Measures*, International Journal of Computer Applications (0975 8887), **27**, 2 pp. 33–41, 2011.
18. P.S.M. BERRY and F.B. BERCOVITCH, *Darkening Coat Colour Reveals Life History and Life Expectancy of Male Thornicrofts Giraffes*, Journal of Zoology, 2012.
19. M. RUSU, H.N. TEODORESCU, *A Method for Image Segmentation based on Histograms – Preliminary Results*, Proc. ICTEI2012 Int. Conf., Kishnew, R. of Moldova, 2012, pp. 351–354.
20. H.N. TEODORESCU, M. RUSU, *Yet Another Method for Image Segmentation based on Histograms and Heuristics*, Computer Science Journal of Moldova, **20**, 2(59), pp. 163–177, 2012.
21. M.M. JLASSI, A. DOUIK, H. MESSAOUD, *Objects Detection by Singular Value Decomposition Technique in Hybrid Color Space: Application to Football Images*. Int. J. of Computers, Communications & Control, **V**, 2, pp. 193–204, 2010.
22. T.N. JANAKIRAMAN, P.V.S.S.R. CHANDRA MOULI, *Image Segmentation using Euler Graphs*. Int. J. of Computers, Communications & Control, **V**, 3, pp. 314–324, 2010.
23. M. AIROUCHE, M. ZELMAT, M. KIDOUUCHE, *Statistical Edge Detectors Applied to SAR Images*. Int. J. of Computers, Communications & Control, Vol. **III**, Suppl. issue: Proceedings IJCCC, pp. 144–149, 2008.
24. S.I. BEJINARIU, F. ROTARU, C.D. NITĂ, *Information Fusion Techniques for Segmentation of Multispectral Images*, Memoirs of the Scientific Sections of the Romanian Academy, Tome XXXV, 2012.

Received July 19, 2012